Parametrical optimization of laser surface alloyed NiTi shape memory alloy with Co and Nb by the Taguchi method

K W Ng, H C Man, J Lawrence and T M Yue

Proceedings of the Institution of Mechanical Engineers, Part B: Journal of Engineering Manufacture 2009 223: 969
DOI: 10.1243/09544054JEM1291

Parametrical optimization of laser surface alloyed NiTi shape memory alloy with Co and Nb by the Taguchi method

K W Ng[1]*, H C Man[1], J Lawrence[2], and **T M Yue[1]**
[1]Advanced Manufacturing Technology Research Centre, The Hong Kong Polytechnic University, Hong Kong
[2]Wolfson School of Mechanical and Manufacturing Engineering, Loughborough University, Leicestershire, UK

The manuscript was received on 8 July 2008 and was accepted after revision for publication on 11 March 2009.

DOI: 10.1243/09544054JEM1291

Abstract: Different high-purity metal powders were successfully alloyed on to a nickel titanium (NiTi) shape memory alloy (SMA) with a 3 kW carbon dioxide (CO_2) laser system. In order to produce an alloyed layer with complete penetration and acceptable composition profile, the Taguchi approach was used as a statistical technique for optimizing selected laser processing parameters. A systematic study of laser power, scanning velocity, and pre-paste powder thickness was conducted. The signal-to-noise ratios (S/N) for each control factor were calculated in order to assess the deviation from the average response. Analysis of variance (ANOVA) was carried out to understand the significance of process variables affecting the process effects. The Taguchi method was able to determine the laser process parameters for the laser surface alloying technique with high statistical accuracy and yield a laser surface alloying technique capable of achieving a desirable dilution ratio. Energy dispersive spectrometry consistently showed that the per cent by weight of Ni was reduced by 45 per cent as compared with untreated NiTi SMA when the Taguchi-determined laser processing parameters were employed, thus verifying the laser's processing parameters as optimum.

Keywords: NiTi, Taguchi method, laser surface alloying

1 INTRODUCTION

Laser alloying has attracted increased industrial attention in recent years owing to the unique characteristics and capabilities of metallic coating for surface properties enhancement. Laser alloying is believed by many to enhance the surface properties of different alloys [**1**–**7**]. To date, many different alloys have been surface-processed using lasers. Surface alloying with chromium (Cr), silicon (Si), or carbon (C) on cast iron was discussed by Belforte *et al.* [**8**]. The carbon alloying of stainless steel has been studied by Marsden *et al.* [**9**]. Surface alloying of aluminium with Si, C, N, and nickel (Ni) has been shown by Walker *et al.* [**10**]. Liu *et al.* [**11**, **12**] suggested that laser surface alloying could become important in making machine-readable coinage. The growing industrial acceptance of the technique drives an increase in concern of the process quality and stability. A study of the fundamental parameters of the laser alloying process would, therefore, be beneficial in the development of the process as a reliable surface modification technology. Adjustable process parameters such as laser power (W), scanning speed (mm/s), and powder paste thickness (mm) have been shown to be most significant in influencing the alloying quality during laser surface treatment [**13**–**16**]. Dubey and Yadava [**17**] and Anawa and Olabi [**18**] reported the successful application of the Taguchi method in laser cutting and laser welding respectively. Raghunath and Pandey [**19**] and Bandyopadhyay *et al.* [**20**] successfully applied the method of analysis of variance (ANOVA) to understand the significance of process variables affecting the properties in laser sintering and laser drilling respectively. Chen and Huang [**21**] employed a self-organizing fuzzy control method to study the Ti6Al4V

*Corresponding author: *Industrial and Systems Engineering, The Hong Kong Polytechnic University, DE404, E Core, 4/F, Hung Hom, Hong Kong.*
email: maggiekwng@gmail.com

laser alloying process. Hitherto no studies have been made to investigate the effect of the laser processing parameters on laser surface alloying using a reliable statistical method. The present work aims to determine the effect of laser processing parameters in laser surface alloyed nickel titanium (NiTi) shape memory alloys (SMAs) (55% wt. Ni–45% wt. Ti) with niobium (Nb) and carbon monoxide (Co) powders with a high level accuracy.

The use of NiTi SMAs has increased in the medical devices industry. The shape memory effect, superelasticity, and good biocompatibility [**22**–**25**] were the driving forces for the early introduction of commercial medical applications [**26**, **27**]. Nb and Co are chosen to be the alloy elements because of their good biocompatibility for medical metals [**28**]. In this work, such coatings are necessary to prevent Ni release (which is toxic) from the NiTi SMA. The Taguchi method is used to analyse the laser parameters – laser power, scan speed, and powder paste thickness – and to obtain the optimum set of laser processing parameters. The penetration ratio and the per cent by weight of Ni of the alloyed layer were determined in order to validate the developed models in terms of optimum level of laser processing parameters.

2 APPLICATION OF THE TAGUCHI METHOD FOR DETERMINING THE PROCESS PARAMETERS

The Taguchi method has been proved to satisfy the needs of problem solving and process parameters optimization in the most economic fashion. The objective of the Taguchi approach is to optimize process control parameters, study the influences of individual factors and their interactions, and to reduce variations in the process quality. This method consequently improves the performance characteristics of the process and controls the process variation. Experimental design is essentially useful in identifying the key decision factors and their associated levels so as to maximize the yield of the process. The factors and levels of significance are identified for the appropriate orthogonal array to study the entire parameter space with a small number of experiments.

2.1 Signal-to-noise ratio

Signal-to-noise (S/N) ratio is employed to quantify the deviation from the desired value. The lower-the-better (LB), the higher-the-better (HB), and the nominal-the-better (NB) are the three categories used to analyse the S/N ratio, η. Different S/N ratios are applicable for particular types of characteristics, but a larger S/N ratio always corresponds to a better performance characteristic. The optimal level of the process parameters is the level with the highest S/N ratio, η, [**29**]. The following equations are usually used to calculate the S/N ratio

$$\textit{Smaller–the–better} : S/N_{\mathrm{S}} = -10\log\left(\frac{1}{n}\sum_{i=1}^{n} y_i^2\right) \tag{1}$$

$$\textit{Larger–the–better} : S/N_{\mathrm{L}} = -10\log\left(\frac{1}{n}\sum_{i=1}^{n}\frac{1}{y_i^2}\right) \tag{2}$$

$$\textit{Nominal–the–best} : S/N_{\mathrm{T}} = 10\log\left(\frac{\bar{y}}{Sy^2}\right) \tag{3}$$

where, $\bar{y}$ is the average of observed data, Sy^2 is the variance of y, n is the number of observations, and y represents the observed data.

2.2 Analysis of variance (ANOVA)

ANOVA is a meticulous statistical procedure employed to analyse data in order to determine their variability. By understanding the source and magnitude of the variance, evidence-based operating conditions can be predicted. The statistical calculation method for the ANOVA process for the laser alloying process under discussion is given as follows [**30**].

The correction factor (CF) means the overall grand mean of all the observations. CF is computed using

$$\mathrm{CF} = \frac{\left(\sum_{i=1}^{p}\sum_{j=1}^{v}\sum_{k=1}^{t} x_{ijk}\right)^2}{n} \tag{4}$$

The total sum of square (SST) represents the total variation among all the observations around the grand mean. SST is computed using

$$\mathrm{SST} = \sum_{i=1}^{p}\sum_{j=1}^{v}\sum_{k=1}^{t}\left(x_{ijk}\right)^2 - \mathrm{CF} \tag{5}$$

The sum of square of power factor (SSp) represents the differences among the various levels of power and the grand mean. SSp is computed using

$$\mathrm{SS}p = \sum_{i=1}^{p}\frac{\left(\sum_{j=1}^{v}\sum_{k=1}^{t} x_{ijk}\right)^2}{n_{\mathrm{v}} n_{\mathrm{t}}} - \mathrm{CF} \tag{6}$$

where n_{v} and n_{t} represent the number of levels of speed factor and powder paste thickness factor respectively.

The sum of square of speed factor (SSv) represents the differences among the various levels of speed and the grand mean. SSv is computed using

$$\mathrm{SS}v = \sum_{j=1}^{v}\frac{\left(\sum_{i=1}^{p}\sum_{k=1}^{t} x_{ijk}\right)^2}{n_{\mathrm{p}} n_{\mathrm{t}}} - \mathrm{CF} \tag{7}$$

Table 1 Analysis of variance (ANOVA) table

Source	Degree of freedom	Sum of square	Mean square	F test	% contribution
Power (p)	n_p-1	SS_p	$MSp = \frac{SSp}{n_p-1}$	$Fp = \frac{MSp}{MSE}$	$\frac{SSp}{SST}\times 100\%$
Speed (v)	n_v-1	SS_v	$MSv = \frac{SSv}{n_v-1}$	$Fv = \frac{MSv}{MSE}$	$\frac{SSv}{SST}\times 100\%$
Powder paste thickness (t)	n_t-1	SS_t	$MSt = \frac{SSt}{n_t-1}$	$Ft = \frac{MSt}{MSE}$	$\frac{SSt}{SST}\times 100\%$
P–v interaction	$(n_p-1)(n_v-1)$	SS_{pv}	$MSpv = \frac{SSpv}{(n_p-1)(n_v-1)}$	$Fpv = \frac{MSpv}{MSE}$	$\frac{SSpv}{SST}\times 100\%$
P–t interaction	$(n_p-1)(n_t-1)$	SS_{pt}	$MSpt = \frac{SSpt}{(n_p-1)(n_t-1)}$	$Fpt = \frac{MSpt}{MSE}$	$\frac{SSpt}{SST}\times 100\%$
V–t interaction	$(n_v-1)\ (n_t-1)$	SS_{vt}	$MSvt = \frac{SSvt}{(n_v-1)(n_t-1)}$	$Fvt = \frac{MSvt}{MSE}$	$\frac{SSvt}{SST}\times 100\%$
Error	e*	SSE	$MSE = \frac{SSE}{e*}$		$\frac{SSE}{SST}\times 100\%$
Total	$n-1$	SST			

*e = total number of df – (sum of the other df) = $(n-1) - (df_1 + df_3 + df_2 + \ldots + df_m)$ where n is the total number of observations and m is the total number of sources for ANOVA calculation

where n_p and n_t represent the number of levels of power factor and powder paste thickness factor respectively.

The sum of square of powder paste thickness factor (SSt) represents the differences among the various levels of powder paste thickness and the grand mean. SSt is computed using

$$SSt = \sum_{k=1}^{t} \frac{\left(\sum_{i=1}^{p}\sum_{j=1}^{v} x_{ijk}\right)^2}{n_p n_v} - CF \tag{8}$$

where n_p and n_v represent the number of levels of powder factor and speed factor respectively.

The sum of square owing to interaction between power and speed (SSpv) represents the interacting effect of specific combinations of power and speed factor. SSpv is computed using

$$SSpv = \sum_{i=1}^{p}\sum_{j=1}^{v} \frac{\left(\sum_{k=1}^{t} x_{ijk}\right)^2}{n_t} - SSp - SSv - CF \tag{9}$$

The sum of square owing to interaction between power and powder paste thickness (SSpt) represents the interacting effect of specific combinations of power and powder paste thickness factor. SSpt is computed using

$$SSpt = \sum_{i=1}^{p}\sum_{k=1}^{t} \frac{\left(\sum_{j=1}^{v} x_{ijk}\right)^2}{n_v} - SSp - SSt - CF \tag{10}$$

The sum of square owing to interaction between powder paste thickness and speed (SSvt) represents the interacting effect of specific combinations of powder paste thickness and speed factor. SSvt is computed using

$$SSvt = \sum_{j=1}^{v}\sum_{k=1}^{t} \frac{\left(\sum_{i=1}^{p} x_{ijk}\right)^2}{n_p} - SSv - SSt - CF \tag{11}$$

The sum of square error (SSE) represents the differences among the observations within each cell and the corresponding cell mean. SSE is computed using

$$SSE = SST - (SSp + SSv + SSt) \tag{12}$$

The mean squares are found by dividing the sum of squares by the corresponding number of degrees of freedom. The F-test is the ratio of the mean squares for treatment to the mean squares for error. The percentage contribution is obtained by dividing the pure sum of squares for that factor by the total sum of square and then multiplying the result by 100. The entire set of steps is summarized in Table 1.

If the F-test value is larger than the standard F-value at 0.01 level of significance (99 per cent confidence) [**31**], the factor is said highly to influence the process response. The credible percentage contribution is collated to determine the variation of each factor for the process. The more marked the percentage contribution value, the more the majority of the factor in question influences the process.

3 EXPERIMENTAL PROCEDURES

3.1 Materials

To remove the oxide layer, 5 mm thick NiTi SMA samples of $50\times 30\,mm^2$ size were mechanically ground with 120 grit SiC paper. The specimens were then ultrasonic cleaned in acetone and sand-blasted for better adhesion with the paste of high-purity Co

Table 2 Thermal properties of Co and Nb powders

Thermal properties	Co	Nb
Melting point (°C)/(K):	1495/1768	2477/2750
Boiling point (°C)/(K):	2927/3200	4744/5017
Thermal conductivity ($W/m\,K^{-1}$)	100	54
Coefficient of linear thermal expansion (K^{-1})	13×10^{6}	7.3×10^{6}

Table 3 Levels of each laser parameter

	Levels of each parameter		
Parameter	Level 1	Level 2	Level 3
Laser power (p) (W)*	600 *(700)*	700 *(800)*	800 *(900)*
Scan speed (v) (mm/min)	600	900	1200
Powder paste thickness (t) (mm)	0.2	0.3	0.4

*The value inside the ( ) are the selected process parameters for Nb-alloyed specimens

Table 4 Experimental array

		Powder paste thickness		
Power	speed	t_1	t_2	t_3
p_1	v_1	$p_1v_1t_1$	$p_1v_1t_2$	$p_1v_1t_3$
	v_2	$p_1v_2t_1$	$p_1v_2t_2$	$p_1v_2t_3$
	v_3	$p_1v_3t_1$	$p_1v_3t_2$	$p_1v_3t_3$
p_2	v_1	$p_2v_1t_1$	$p_2v_1t_2$	$p_2v_1t_3$
	v_2	$p_2v_2t_1$	$p_2v_2t_2$	$p_2v_2t_3$
	v_3	$p_2v_3t_1$	$p_2v_3t_2$	$p_2v_3t_3$
p_3	v_1	$p_3v_1t_1$	$p_3v_1t_2$	$p_3v_1t_3$
	v_2	$p_3v_2t_1$	$p_3v_2t_2$	$p_3v_2t_3$
	v_3	$p_3v_3t_1$	$p_3v_3t_2$	$p_3v_3t_3$

p_1, v_1, and t_1 represent the parameters in level 1; p_2, v_2, and t_2 represent the parameters in level 2, p_3, v_3, and t_3 represent the parameters in level 3; as shown in Table 3

powders (average particle ~35 μm) and Nb powders (average particle ~35 μm). Co and Nb powders were mixed with polyvinyl alcohol (PVA) to form pastes which were then applied to the NiTi SMA surface. The thermal properties of the Co and Nb powders are listed in Table 2.

3.2 Laser surface alloying procedures

A laser surface alloying process is selected for enhancing the surface properties of NiTi SMA as it does not affect the shape memory properties of the NiTi SMA; indeed, it is perhaps the only process capable of doing this. A continuous wave (CW) 3 kW carbon dioxide (CO_2) laser (PRC Lasers Corporation) was used to surface alloy the Co and Nb onto the surface of the NiTi. In general, there are numerous parameters that need to be considered for the laser surface alloying process, such as laser power, scanning speed, gas flowrate, beam diameter, focal length, and powder paste thickness. However, previous works have shown power, speed, and powder paste thickness to be of most influential in terms of alloy quality [**13–16**]. To obtain the optimum laser processing parameters in this work, selected laser parameters were systemically varied; laser power, p, in the range of 600 to 900 W, scanning speed, v, in the range of 600 to 1200 mm/min, and powder paste thickness, t, in the range of 200 to 400 μm. In view of previous work [**13–16**], other parameters have been kept constant throughout the experiment. Table 3 shows the process parameters and the ranges studied. The upper laser power level for Nb-alloyed specimens was selected to be 100 W higher than that for Co-alloyed specimens because of the higher melting point of Nb (melting point of Nb: 2750K; melting point of Co: 1760K). A combination of three process parameters resulted in a total number of 27 experiments with nine rows and three columns, as shown in Table 4, in which, p_1, v_1, and t_1 represents the parameters in level 1, p_2, v_2, and t_2 represents the parameters in level 2, etc., as shown in Table 3. After laser alloying, Co and Nb have been successfully alloyed on the NiTi, the interface is of metallurgical nature and no crack nor porosity was found in both layers. The alloyed-samples were sectioned, mounted, and polished using 1 μm diamond paste. The cross-section was etched with reagent (HF 10%, HNO_3 40%, H_2O 50%) to aid observation of the melt depth under an optical microscope.

3.3 Analysis of experimental data procedure

Dilution ratio (DR) is generally considered to be one of the key factors governing the mechanical and corrosion properties of a laser alloyed material. Because this work requires t to be considered, the DR of the laser alloyed NiTi SMA in this work was calculated using [**2**]

$$\mathrm{DR} = \left(1 - \frac{t}{d}\right) \tag{13}$$

where t is the powder paste thickness and in the range 200–400 μm and d is the total laser melt depth in the substrate. A schematic diagram of the DR equation variables is given in Fig. 1.

The composition profile for each sample after laser alloying with either Nb or Co experiment was acquired by energy dispersive spectrometry (EDS) (Leica Stereo-scan 440; Leica Microsystems, GmbH) to identify the elemental weight of Ni. A relatively low Ni content is desirable as it will greatly alleviate the risk of Ni ion release into the human body and thus avoid allergic reactions after medical application.

The reason for noting amount of Ni in the alloyed layer is that Ni is a toxic element which will reduce the biocompatibility of the NiTi. The DR is used to qualify the penetration of the alloyed layer. The aim of the present work is to determine which parameter and the extent to which one affects the amount of Ni and dilution ratio most significantly. The relationship between the amount of Ni and dilution is not the main focus of this work.

4 RESULTS

The experimental data for the DR and the per cent by weight of Ni for Co-alloyed and Nb-alloyed specimens are shown in Tables 5 and 6 respectively. The statistical results are from calculations based on the measured experimental data.

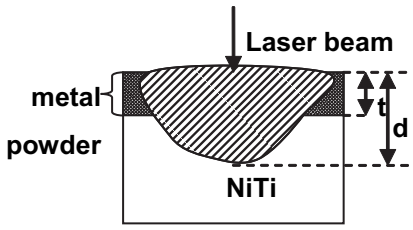

Fig. 1 A schematic diagram of the DR calculation

4.1 Signal-to-noise ratio analysis

The S/N ratio for each control factor was calculated to evaluate the influence of each selected factor on the responses. The signals indicated the effect on the average responses and the noises were measured as deviations from the average responses. The appropriate S/N ratio should be carefully chosen depending on the project objective. In this study the first objective is to obtain the complete penetration of the alloyed layer in which complete penetration is determined by the lowest DR, according to equation (13). The second objective is a reduction in the per cent by weight of Ni as this is desirable for medical application. The smaller-the-better for S/N ratio was chosen in order to minimize the responses for both DR and per cent by weight of Ni.

Table 7 and Table 8 show the corresponding S/N ratio for DR and per cent by weight of Ni of the co-alloyed specimens and Nb-alloyed specimens respectively according to equation (1). The factor effect

Table 5 Experimental data for laser melt depth, dilution ratio and per cent by weight of Ni for Co-alloyed specimens

		Melt depth (μm)			Dilution ratio			Per cent by weight of Ni		
Co-alloyed specimens		Powder paste thickness								
Power	Speed	t_1	t_1	t_2	t_3	t_2	t_3	t_1	t_1	t_2
p_1	v_1	477	599	626	0.68	0.50	0.36	38.64	35.13	19.20
	v_2	529	555	571	0.62	0.46	0.30	38.16	34.24	26.23
	v_3	486	537	515	0.59	0.44	0.22	37.54	33.46	30.44
p_2	v_1	517	586	500	0.61	0.49	0.20	36.56	35.91	34.62
	v_2	507	572	550	0.61	0.48	0.27	39.16	33.10	28.71
	v_3	495	560	586	0.60	0.46	0.32	37.06	31.78	21.50
p_3	v_1	535	684	653	0.63	0.56	0.39	39.44	40.42	37.21
	v_2	532	629	636	0.62	0.52	0.37	39.34	37.64	35.65
	v_3	532	583	605	0.62	0.49	0.34	39.30	34.97	32.50

Table 6 Experimental data for laser melt depth, dilution ratio and per cent by weight of Ni for Nb-alloyed specimens

		Melt depth (μm)			Dilution ratio			Per cent by weight of Ni		
Nb-alloyed specimens		Powder paste thickness								
Power	Speed	t_1	t_1	t_2	t_3	t_2	t_3	t_1	t_1	t_2
p_1	v_1	293	305	474	0.32	0.02	0.16	17.14	20.16	18.73
	v_2	369	406	403	0.46	0.26	0.01	24.75	17.19	26.54
	v_3	307	420	410	0.35	0.28	0.02	18.78	18.80	21.42
p_2	v_1	393	374	419	0.49	0.20	0.05	26.55	13.03	18.92
	v_2	317	541	371	0.37	0.45	−0.08	19.96	29.37	21.41
	v_3	395	429	419	0.49	0.30	0.05	26.66	19.80	22.01
p_3	v_1	427	291	565	0.53	−0.03	0.29	33.33	27.65	28.71
	v_2	351	532	490	0.43	0.44	0.18	37.33	28.81	23.22
	v_3	220	500	445	0.09	0.40	0.10	34.98	26.40	15.44

Table 7 S/N responses table for DR and per cent by weight of Ni for Co-alloyed specimens

Measuring items	Factors	Mean S/N ratios for Co-alloyed specimens		
		Level 1	Level 2	Level 3
DR	Speed (v)	6.8224	6.8639	6.9550*
	Power (p)	7.2998*	7.2118	6.1582
	Powder paste thickness (t)	4.3130	6.2403	10.4236*
Per cent by weight Ni	Speed (v)	−30.7706	−30.7291*	−30.7588
	Power (p)	−30.0741*	−30.7485	−31.4347
	Powder paste thickness (t)	−31.6738	−30.9063	−29.2218*

*Optimum level for Co-alloyed specimens

Table 8 S/N responses table for DR and per cent by weight of Ni for Nb-alloyed specimens

Measuring items	Factors	Mean S/N ratios for Nb-alloyed specimens		
		Level 1	Level 2	Level 3
DR	Speed (v)	17.2485*	14.3336	14.7599
	Power (p)	19.5740*	12.6604	13.8744
	Powder paste thickness (t)	8.9607	15.0366	23.6696*
Per cent by weight of Ni	Speed (v)	−26.7774*	−27.8876	−26.8885
	Power (p)	−26.0955*	−26.5935	−28.8317
	Powder paste thickness (t)	−28.2004	−26.7034	−26.6458*

*Optimum level for Nb-alloyed specimens

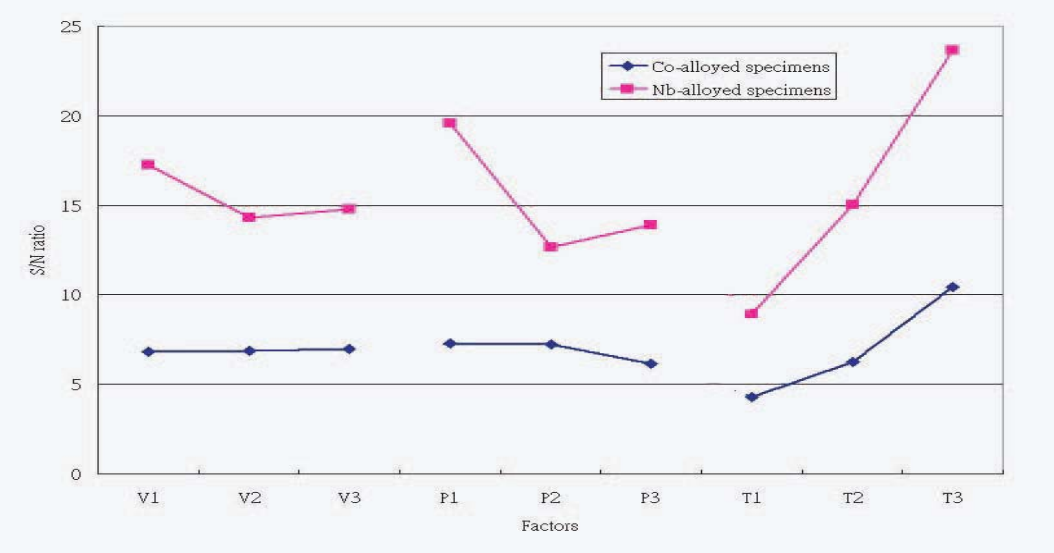

Fig. 2 Dilution ratio responses graphs for factor level on S/N ratio

of a parameter at any level is computed by taking the average of all S/N ratios at the same level. The graphical representations of the factors effect at different levels are shown in Fig. 2 (DR) and Fig. 3 (per cent by weight of Ni). The optimum parameter level is the level corresponding to the maximum average S/N ratio for a control factor. So, from Figs 2 and 3, it is evident that the optimum parameter levels for minimum values of DR and per cent by weight of Ni for co-alloyed specimens are $v_3p_1t_3$ and $v_2p_1t_3$ respectively. For Nb-alloyed specimens, Figs 2 and 3 show that the optimum parameters for both DR and per cent by weight of Ni are the same at $v_1p_1t_3$.

4.2 Analysis of variance (ANOVA)

Four sets of ANOVA tables were interpreted to identify the variance of each of the 27 laser process parameters (see Table 4). The collated F-test value and per cent contribution for the measured DR

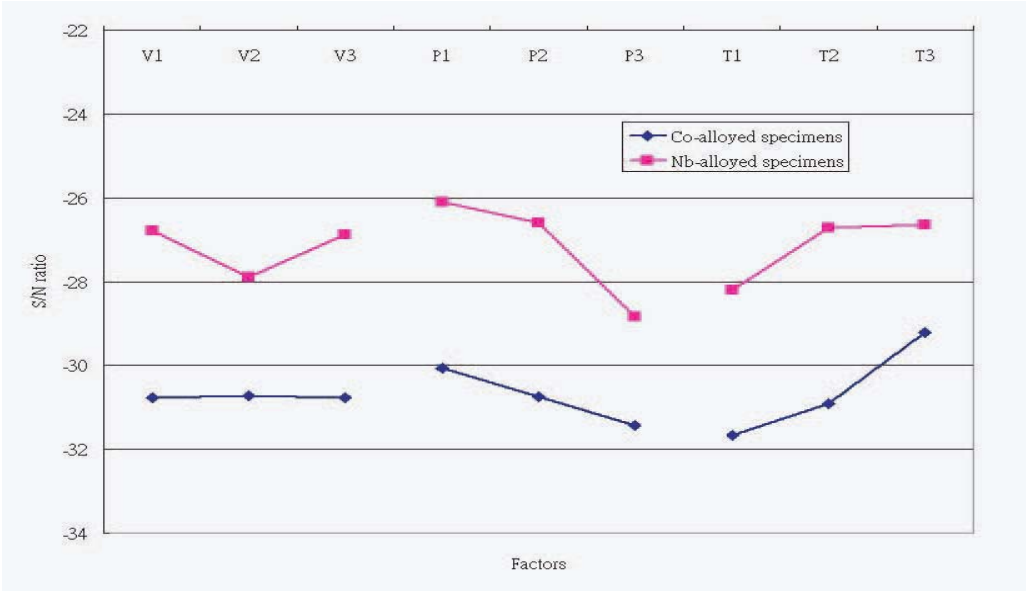

Fig. 3 Weight % of Ni responses graphs for factor level on S/N ratio

Table 9 ANOVA table for the DR of Co-alloyed specimens

Source	Sum of square	df	Mean square	F test	F	% contribution
v	0.0033	2	0.0017	1.1354	10.11	0.4063
p	0.0177	2	0.0089	6.0301	10.11	3.5362
t	0.4130	2	0.2065	140.4422	10.11	89.4851*
v–*p* interaction	0.0064	4	0.0016	1.0882	7.96	1.0719
v–*t* interaction	0.0021	4	0.0005	0.3542	7.96	0.1332
t–*p* interaction	0.0056	4	0.0014	0.9468	7.96	0.8911
Residual	0.0118	8	0.0015	–	–	2.8775
Total	0.4599	26	–	–	–	–

*The major factor(s) influence the DR of Co-alloyed specimens

Table 10 ANOVA table for the weight of Ni of Co-alloyed specimens

Source	Sum of square	df	Mean square	F test	F	% contribution
v	20.5848	2	10.2924	0.8008	10.11	2.8008
p	124.5606	2	62.2803	4.8458	10.11	16.9479
t	357.1507	2	178.5754	13.8944	10.11	48.5944*
v–*p* interaction	57.4510	4	14.3627	1.1175	7.96	7.8168
v–*t* interaction	11.0552	4	2.7638	0.2150	7.96	1.5042
t–*p* interaction	61.3427	4	15.3357	1.1932	7.96	8.3464
Residual	102.8186	8	12.8523	–	–	13.9896
Total	734.9635	26	–	–	–	–

*The major factor(s) influence the weight of Ni of Co-alloyed specimens

(equation (13)) and per cent by weight of Ni of co-alloyed specimens and Nb-alloyed specimens are given in Tables 9, 10 and 11, 12 respectively.

The 0.01 level of significance is evaluated to determine whether there is evidence of an interaction effect. The approximate upper-tail critical value from the F distribution with four degrees of freedom in the numerator and eight degrees of freedom in the denominator is 7.96. Because all $F_{ij} < F_U = 7.96$ (Tables 9 to 12), there is insufficient evidence of an interacting effect between power, scan speed, and powder paste thickness, as well as combinations thereof. As such, it is possible to neglect the interaction parameters and focus only on individual effect.

The 0.01 level of significance is evaluated to test for a difference between each factor. The approximate upper-tail critical value from the F distribution with two degrees of freedom in the numerator and

Table 11 ANOVA table for DR of Nb-alloyed specimens

Source	Sum of square	df	Mean square	F test	F	% contribution
v	0.0158	2	0.0079	0.5598	10.11	1.7540
p	0.0194	2	0.0097	0.6899	10.11	2.1618
t	0.4229	2	0.2114	15.0076	10.11	47.0264*
v–p interaction	0.0316	4	0.0079	0.56043	7.96	3.5121
v–t interaction	0.2194	4	0.0548	3.8919	7.96	24.3905
t–p interaction	0.0775	4	0.0194	1.3756	7.96	8.6212
Residual	0.1127	8	0.0142	–	–	12.5340
Total	0.8993	26	–	–	–	–

*The major factor(s) influence the DR of Nb-alloyed specimens

Table 12 ANOVA table for per cent by weight of Ni of Nb-alloyed specimens

Source	Sum of square	df	Mean square	F test	F	% contribution
v	43.8794	2	21.9397	0.7919	10.11	4.5895
p	326.5647	2	163.2824	5.8938	10.11	34.1565*
t	123.7057	2	61.8529	2.2326	10.11	12.9388
v–p interaction	48.5198	4	12.1299	0.4378	7.96	5.0748
v–t interaction	23.4971	4	5.8743	0.2120	7.96	2.4576
t–p interaction	168.2856	4	42.0714	1.5186	7.96	17.6016
Residual	221.6311	8	27.7039	–	–	23.1812
Total	956.0834	26	–	–	–	–

*The major factor(s) influence the per cent by weight of Ni of Nb-alloyed specimens

eight degrees of freedom in the denominator is 10.11. For those factor(s) where $F_i < F_U = 10.11$, it can be concluded that there is insufficient evidence of a difference between three levels of each factor for the particular evaluated result(s). In contrast, for those factor(s) where $F_i < F_U = 10.11$, it can be concluded that there is sufficient evidence of a difference between three levels of each factor for the particular evaluated result(s).

The major factor(s) that influence the variations of the factors' performance are indicated in the 'contribution' column in Tables 9, 10, 11, and 12. According to the experimental data shown in Tables 5 and 6, the preliminary findings between the parameters and factors can be enumerated as outlined below.

1. The average melt depth of the laser treated zone decreased with increasing scan speed from 600 mm/min to 1200 mm/min.
2. The average treated zone of the Co-alloyed specimens increased for the depth from 543 μm to 599 μm with an increase in laser power from level 1 to level 3. The average treated zone of the Nb-alloyed specimens increased for the depth from 376 μm to 425 μm with an increase in laser power from level 1 to level 3.
3. The DR decreased linearly for an increase in powder paste thickness. The DR decreased 50 per cent for an increase in scan speed from 0.2 mm to 0.4 mm.
4. Powder paste thickness is the most significant parameter affecting the DR and per cent by weight of Ni. The lowest value of Ni content is generated with a 0.4 mm powder paste thickness.

5 DISCUSSION

From the ANOVA analysis the melt depth was observed to decrease with increasing scan speed. This is probably the result of reduced interaction time between the specimen surface and the laser beam as it moves over the surface with increased scan speed. The effect of both laser power and scan speed on the melt depth can be explained by specific energy (E_{specific}) [**1**]

$$E_{\text{specific}} = \frac{P}{2rv} \tag{14}$$

where P is the laser power (W), v is the process speed (mm/min), and r is the laser spot radius on the substrate surface (mm).

In this work the laser spot radius was set at 1.5 mm throughout all the experiments. According to equation (14) the slower the scan speed and the larger the power, the larger the energy provided to the surface of a sample; thus larger energy absorption naturally results in a thicker melt depth.

It is clear from Tables 5 and 6 that there is a reduction in DR and a significant drop in per cent by weight of Ni as the powder paste thickness is

increased. The relationship between the DR and powder paste thickness is evident from equation (13); therefore a reduction in DR means that more alloyed powders were integrated with the base substrate under the same conditions.

The optimum level of the laser processing parameters is the level with the highest S/N ratio. According to Figs 2 and 3 the optimum laser processing parameter levels for minimum values of DR and per cent by weight of Ni for co-alloyed specimens are $v_3p_1t_3$ and $v_2p_1t_3$ respectively. For Nb-alloyed specimens the optimum laser processing parameters for both DR and per cent by weight of Ni are the same at $v_1p_1t_3$. As mentioned earlier, higher power is necessary for alloying Nb on NiTi SMA because Nb has a higher melting point than Co; therefore it requires more energy in initiate melting. Table 10 shows that the per cent contribution of speed for the laser alloying of Co was insignificant. So, because speed is not the most influential factor for Co-alloyed specimens, and as the S/N ratio maintained at a relatively constant level (see Table 7), the optimum speed level could be randomly chosen without having a significant effect on the performance; accordingly the fastest speed, v_3, was selected so as to increase the production efficiency. By comparing the data in Tables 7 and 8, Nb-alloyed specimens always achieved a higher S/N ratio than those of Co. Nb is therefore considered as a relatively controllable alloying element. As the laser alloying processing conditions are similar for both Co powder and Nb powder, Nb is assumed to be the potential alloying material for NiTi SMA owing to better alloying efficiency.

ANOVA indicated that powder paste thickness is the most influential factor for both alloying metal powders. According to Tables 9 and 10, the contribution percentage for the factor of powder paste thickness in Co-alloyed specimens dominated 90 per cent and 50 per cent for the DR and per cent by weight of Ni respectively. The contribution percentage for Nb-alloyed specimens, however, was less at 45 per cent and 10 per cent for the DR and the per cent by weight of Ni respectively only, as shown in Tables 11 and 12. This large difference in the contribution percentage for the same influence factor could be down to the different physical properties of each metal powder. Indeed the thermal conductivity of Co (100 W/mK) is almost twice that of Nb (53 W/mK) as the same thicknesses of Nb and Co metal powder was pasted onto the NiTi SMA sample surfaces, then the high thermal conductivity of the Co will cause the metal powder on the surface to conduct the heat generated from the laser energy to the bottom more quickly and will result in a larger melt depth. Thus, over penetration with a larger DR of Co-alloyed specimens can be attributed to the higher thermal conductivity of Co powder.

It is somewhat surprising that for laser alloying, the power and the scan speed are not the most influential factors, because for other laser processing, such as laser cutting and laser welding, power and scan speed are always considered as the major factors affecting the output performance. The fact that laser power and scan speed play a smaller role in laser alloying is perhaps due to there being more than one material being processed: laser alloying routinely requires different types of materials to form a homogeneous layer on the substrate surface. The properties of the selected materials, such as thermal conductivity, thermal expansion, density, and melting point, will directly affect the alloyed zone performance, and so the level of influence of the material selection is much higher than the power and speed factors.

The results obtained for the different alloying materials used in this work, Co and Nb, demonstrated desirable statistical accuracy. It is therefore possible to assert that the Taguchi method is repeatable and reliable in determining the optimum laser processing parameters and reduce the process variation in laser surface alloying with these materials.

6 CONCLUSIONS

This paper has presented an application of the parameter design of the Taguchi method in the optimization of laser surface alloying. Conclusions can be drawn based on the experimental results of this study.

1. Among the selected process parameters, powder paste thickness has the strongest effect on the dilution ratio and per cent by weight of Ni.
2. Laser power and scanning speed are not considered as the most influential factors in the laser surface alloying process.
3. The optimum parameter levels with the objectives of minimum value DR and per cent by weight of Ni for Co- and Nb-alloyed specimens are $v_3p_1t_3$ and $v_1p_1t_3$ respectively.
4. Co and Nb were successfully alloyed onto the surfaces of NiTi SMA samples and achieved a desirable dilution ratio of 0.3 and 0.1 respectively. The per cent by weight of Ni was seen to be reduced from an as-received value of 55 per cent to 38 per cent for Co-alloyed specimens and 26 per cent for Nb-alloyed specimens.

ACKNOWLEDGEMENT

The author would like to acknowledge the Hong Kong Polytechnic University for the provision of facilities and a research grant for K W Ng (Project No: RGER).

REFERENCES

1 **Steen, W. M.** *Laser material processing*, 1991 (Springer-Verlag, New York).
2 **Man, H. C., Ho, K. L.,** and **Cui, Z. D.** Laser surface alloying of NiTi shape memory alloy with Mo for hardness improvement and reduction of Ni2+ ion release. *Surface Coatings Technol.*, 2006, **200**(14–15), 4612–4618.
3 **Ng, K. W., Man, H. C., Cheng, F. T.,** and **Yue, T. M.** Laser cladding of copper with molybdenum for wear resistance enhancement in electrical contacts. *Appl. Surface Sci.*, 2007, **253**(14), 6236–6241.
4 **Tian, Y. S., Chen, C. Z., Li, S. T.,** and **Huo, Q. H.** Research progress on laser surface modification of titanium alloys. *Appl. Surface Sci.*, 2005, **242**(1–2), 177–184.
5 **Jiang, P., He, X. L., Li, X. X., Yu, L. G.,** and **Wang, H. M.** Wear resistance of a laser surface alloyed Ti-6Al-4V alloy. *Surface Coatings Technol.*, 2000, **130**(1), 24–28.
6 **García, I.** and **Damborenea, J. J. D.** Corrosion properties of tin prepared by laser gas alloying of Ti and Ti6Al4V. *Corrosion Sci.*, 1998, **40**(8), 1411–1419.
7 **Carvalho, P. A.** and **Vilar, R.** Laser alloying of zinc with aluminum: solidification structures. *Surface Coatings Technol.*, 1997, **91**(3), 158–166.
8 **Belforte, D.** and **Levitt, M.** *Laser surface melting of cast irons and alloy cast irons*. In Industrial laser annual handbook (Eds W. M. Steen, Z. D. Chen, and D. R. F. West), 1987, pp. 80–96 (Laser Institute of American).
9 **Marsden, C., West, D. R. F.,** and **Steen, W. M.** Laser surface alloying of stainless steel with carbon. Proceedings of NATO Advanced Study Institute on *Laser surface treatment of metals* (Eds C. W. Draper and P. Mazzoldi), 1986, pp. 461–474 (Martinus Nijhoff, Dordrecht, Netherlands).
10 **Walker, A. M., West, D. R. F.,** and **Steen, W. M.** Laser surface alloying ferrous materials with carbon. Proceeding of Laser'83 Optoelectronik Conference (ed. W. Waidelich), Munich, 1983, pp. 322–326.
11 **Liu, Z., Watkins, K. G.,** and **Steen, W. M.** An analysis of broken-layer characteristics in laser alloying for coinage applications. *J. Laser Applic.*, 1999, **11**(3), 136–142.
12 **Liu, Z., Pirch, N., Gasser, A., Watkins, K. G.,** and **Hatherley, P. G.** Effect of beam width on melt characteristics in large area surface alloying. *J. Laser Applic.*, 2001, **13**(6), 231–238.
13 **Kumar, V. C.** Process parameters influencing melt profile and hardness of pulsed laser treated Ti-6Al-4V. *Surface and Coatings Technol.*, 2006, **201**(6), 3174–3180.
14 **Ozegowski, M., Metev, S.,** and **Sepold, G.** Influence of laser parameters on the formation of ablative plasma fluxes and the properties of deposited thin films. *Appl. Surface Sci.*, 1998, 127–129, 614–619.
15 **Srivastava, D., Chang, I. T. H.,** and **Loretto, M. H.** The optimisation of processing parameters and characterisation of microstructure of direct laser fabricated TiAl alloy components. *Mater. Des.*, 2000, **21**(4), 425–433.
16 **Rana, J., Goswami, G. L.,** and **Jha, S. K.** *et al.* Experimental studies on the microstructure and hardness of laser-treated steel specimens. *Optics Laser Technol.*, 2007, **39**(2), 385–393.
17 **Dubey, A. K.** and **Yadava, V.** Multi-objective optimization of Nd:YAG laser cutting of nickel-based superalloy sheet using orthogonal array with principal component analysis. *Optics Lasers Engng*, 2008, **46**(2), 124–132.
18 **Anawa, E. M.** and **Olabi, A. G.** Using Taguchi method to optimize welding pool of dissimilar laser-welded components. *Optics Laser Technol.*, 2008, **40**(2), 379–388.
19 **Raghunath, N.** and **Pandey, P. M.** Improving accuracy through shrinkage modelling by using Taguchi method in selective laser sintering. *Int. J. Machine Tools Mf.*, 2007, **47**(6), 985–995.
20 **Bandyopadhyay, S., Gokhale, H., Sarin Sundar, J. K., Sundararajan, G.,** and **Joshi, S. V.** A statistical approach to determine process parameter impact in Nd:YAG laser drilling of IN718 and Ti-6Al-4V sheets. *Optics and Lasers Engng*, 2005, **43**(2), 163–182.
21 **Chen, H.-Y.** and **Huang, S.-J.** Ti6A14V laser alloying process control by using a self-organizing fuzzy controller. *Int. J. Machine Tools Mf.*, 2004, **44**(15), 1653–1665.
22 **Castleman, L. S., Motzkin, S. M., Alicandri, F. P., Bonawit, V. L.,** and **Johnson, A. A.** Biocompatibility of nitinol alloy as an implant material. *J. Biomedical Mater. Res.*, 1976, **10**, 695–731.
23 **Prince, M. R., Salzman, E. W., Schoen, F. J., Palestrant, A. M.,** and **Simon, M.** Local intravascular effects of the nitinol wire blood clot filter. *Investigative Radiology*, 1988, **23**, 294–300.
24 **Kasano, F.** and **Morimitsu, T.** Utilization of nickel-titanium shape memory alloy for stapes prosthesis. *Auris Nasus Larynx*, 1997, **24**(2), 137–142.
25 **Ryhänen, J., Kallioinen, M., Serlo, W., Perämäki, P., Junila, J., Sandvik, P., Niemelä, E.,** and **Tuukkanen, J.** Bone healing and mineralization, implant corrosion, and trace metals after nickel-titanium shape memory metal intramedullary fixation. *J. Biomedical Mater. Res.*, 1999, **47**, 472–480.
26 **Gil, F. J.** and **Planell, J. A.** Shape memory alloys for medical applications. *Proc. IMech, Part H: J. Engineering Medicine*, 1998, **212**(H6), 473–488. DOI: 10.1243/0954411981534231.
27 **Shabalovskaya, S. A.** On the nature of the biocompatibility and on medical applications of NiTi shape memory and superelastic alloys. *Biomedical Mater. Engng*, 1996, **6**, 267–289.
28 **Helsen, J. A.** and **Breme, H. J.** *Metals as biomaterials*, 1998 (John Wiley, New York).
29 **Nalbant, M., Gokkaya, H.,** and **Sur, G.** Application of Taguchi method in the optimization of cutting parameters for surface roughness in turning. *Mater. Des.*, 2007, **28**(4), 1379–1385.
30 **Berenson, M. L., Timothy, D. M. L.,** and **Krehbiel, C.** *Basic business statistics: concepts and applications*, 2004 (Prentice Hall, Englewood Cliffs, New Jersey).
31 **Roy, R. K.** *A primer on the Taguchi method*, 1990 (Van Nostrand Reinhold, New York).

APPENDIX 1

Notation

CF	correction factor
d	laser melt depth
df	degree of freedom
F_i	F test for factor i effect
F_{ij}	F test for factor i and j interaction
MS_i	mean square of factor i
MS_{ij}	mean square of factor i and j interaction
n	total number of observations in the experiment (where $n = pvt$)
n_p	number of levels of power factor
n_v	number of levels of speed factor
n_t	number of levels of powder paste thickness factor
p	power
r	laser spot radius
SSE	sum of square error
SST	total sum of square
SS_i	sum of square of factor i
SS_{ij}	sum of square of i and j interaction
t	powder paste thickness
v	speed